Rock and Soil Mechanics

Volume 42 | Issue 11 Article 7

2-23-2022

Reliability analysis of slope and random response of anti-sliding pile considering spatial variability of rock mass properties

Wen-gang ZHANG
National Joint Engineering Research Center of Geohazards Prevention in the Reservoir Areas, Chongqing University, Chongqing 400045, China

Qi WANG
School of Civil Engineering, Chongqing University, Chongqing 400045, China

Fu-yong CHEN
School of Civil Engineering, Chongqing University, Chongqing 400045, China

Long-long CHEN
School of Civil Engineering, Chongqing University, Chongqing 400045, China

See next page for additional authors

Custom Citation

ZHANG Wen-gang, WANG Qi, CHEN Fu-yong, CHEN Long-long, WANG Lu-qi, WANG Lin, ZHANG Yan-mei, WANG Yu-qi, ZHU Xing, . Reliability analysis of slope and random response of anti-sliding pile considering spatial variability of rock mass properties[J]. Rock and Soil Mechanics, 2021, 42(11): 3157-3168.

Reliability analysis of slope and random response of anti-sliding pile considering spatial variability of rock mass properties

Authors

Wen-gang ZHANG, Qi WANG, Fu-yong CHEN, Long-long CHEN, Lu-qi WANG, Lin WANG, Yan-mei ZHANG, Yu-qi WANG, and Xing ZHU

Rock and Soil Mechanics 2021 42(11): 3157−3168 ISSN 1000−7598
https: //doi.org/10.16285/j.rsm.2021.5464 rocksoilmech.researchcommons.org/journal

Reliability analysis of slope and random response of anti-sliding pile considering spatial variability of rock mass properties

ZHANG Wen-gang[1, 2, 3], WANG Qi[2], CHEN Fu-yong[2], CHEN Long-long[2], WANG Lu-qi[2], WANG Lin[2], ZHANG Yan-mei[4], WANG Yu-qi[5], ZHU Xing[6]

1. Key Laboratory of New Technology for Construction of Cities in Mountain Area, Chongqing University, Chongqing 400045, China
2. School of Civil Engineering, Chongqing University, Chongqing 400045, China
3. National Joint Engineering Research Center of Geohazards Prevention in the Reservoir Areas, Chongqing University, Chongqing 400045, China
4. College of Aerospace Engineering, Chongqing University, Chongqing 400044, China
5. China Railway 19th Bureau Group Sixth Engineering Co. Ltd, Wuxi, Jiangsu 214028, China
6. State Key Laboratory of Geohazard Prevention and Geoenvironment Protection, Chengdu University of Technology, Chengdu, Sichuan 610059, China

Abstract: In the reliability analysis of slope stability, the deterministic analysis method is usually used to calculate the safety factor to evaluate the stability of slope. However, the inherent spatial variability of rock mass properties cannot be considered and described adequately in traditional deterministic method, resulting in the inaccurate calculation of slope failure probability. Based on Hoek-Brown criterion and random finite difference method (RFDM), the reliability analysis of slope stability and random response of pile are discussed in this paper considering spatial variability of rock mass. The uniaxial compressive strength σ_{ci} and material constant for the intact rock m_i are regarded as random field variables and geological strength index GSI is assumed to be a random variable. The results show that the spatial variability of rock mass parameters has a significant effect on slope failure probability and pile response. Ignoring the spatial variability of rock mass parameters will overestimate slope failure probability and the mean value of the maximum bending moment of anti-slide pile, and underestimate the mean value of displacement at pile head. The results can provide design guidance for slope reinforcement as well as layout optimization of anti-sliding piles.

Keywords: reliability assessment of slopes; spatial variability; Hoek-Brown criterion; random finite difference method (RFDM); random response

1 Introduction

Geotechnical parameters have significant spatial variability due to differences in depositional conditions, loading history and other geological effects. And the geotechnical parameters at different spatial locations are somewhat correlated and not completely independent, which makes the slope stability research work more complicated[1−2]. However, the traditional deterministic analysis often evaluates the stability of slopes by the safety factor [3]. The uncertainty about the geotechnical parameters and the relative importance of the geotechnical parameters to the slope stability cannot be fully considered[4−7], which leads to the failure of some slopes even though the safety factor is high[8]. Therefore, in order to further understand the influence of spatial variability of geotechnical parameters on engineering reliability, random fields are often used to describe the naturally existing spatial variability of geotechnical bodies before performing slope reliability analysis. Probabilistic methods are often used as a means to effectively assess slope reliability when considering geotechnical uncertainties[9], among which Monte Carlo simulation methods are widely used[10]. There have been studies combining the random finite element method (RFEM)[11] and random finite difference method (RFDM)[12] with Monte Carlo simulation methods to study the influence of spatial variability of geotechnical bodies on slope reliability.

In order to reduce the loss caused by slope instability, anti-slide piles are used in engineering to reinforce the slope. Anti-slide pile is a kind of lateral load-bearing pile, which can mobilize the strata far beyond the range of the pile to resist sliding together with it and reinforce the resistance of the strata under the action of landslide thrust. In recent years, some scholars have conducted in-depth studies on the impact of spatial variability on engineering stability and pile foundation response uncertainty. Huang et al.[13] proposed a method for evaluating the stability of anti-slide pile-reinforced slopes based on the reliability theory, which combines the strength reduction method with the response surface method to calculate the probability of slope failure. Teixeira et al.[14] analyzed the reliability of vertically loaded piles using the first-order reliability method and Monte Carlo simulation method, respectively. Chen et al.[15] discussed the influence of anti-slide pile position and pile length on the slope failure probability based on the limit equilibrium method when considering the spatial variability of soil, and analyzed the slope

Received: 13 May 2021 Revised: 18 August 2021
This work was supported by the National Key R&D Program of China (2019YFC1509605) and the Program of China Scholarships Council (201906050026) and the National Natural Science Foundation of China (51778092).
First author: ZHANG Wen-gang, male, born in 1983, PhD, Professor, doctoral supervisor, research interests: geotechnical engineering reliability and risk control. E-mail: zhangwg@cqu.edu.cn
Corresponding author: ZHANG Yan-mei, female, born in 1982, PhD, Associate Professor, research interests: mechanics theory analysis, finite element numerical simulation. E-mail: zhangym@cqu.edu.cn

failure mode. Gong et al.[16] proposed an optimized design framework, while considering the effects of geotechnical spatial variability, model uncertainty and structural parameter uncertainty on the design. Luo et al.[17] discussed the effect of vertical spatial variability of soil parameters on the design of individual energy piles for load carrying capacity limit states and normal use limit states based on the load transfer method and RFDM. It was found that neglecting the spatial variability of the soil will overestimate the failure probability of energy piles in both limit states. From the above analysis, it is clear that most of the research results on the influence of spatial variability of geotechnical bodies on engineering stability and pile foundations are based on the Mohr-Coulomb criterion for soil bodies. There is a lack of research on the reliability of rocky slopes and the random response of piles after anti-slide pile reinforcement.

Since the Hoek-Brown criterion has the advantage of well reflecting the nonlinear damage characteristics and mechanisms of rock masses and conforms to the deformation and damage characteristics of jointed rock masses. In this paper, a study on the random field description parameters (coefficient of variation, correlation coefficient and scale of fluctuation) on the failure probability of rocky slopes before and after anti-slide pile reinforcement and the random response of anti-slide piles was carried out, based on Hoek-Brown criterion and RFDM. Uniaxial compressive strength σ_{ci} and material constant for the intact rock m_i were considered as random field variables, and geological strength indicators were considered as random variables. This can provide a reference for the design of anti-slide piles.

2 RFDM based on Hoek-Brown criterion

2.1 Hoek-Brown criterion

The Hoek-Brown criterion[18] has become one of the most widely used criteria in the field of rock strength prediction and stability analysis. One of its features is the realization of regularizing the rock stress components in a certain mathematical way and relating them to the material properties of the rock mass. Meanwhile, the generalized Hoek-Brown criterion can be expressed both in the form of principal stresses and in the form of positive and shear stresses on the damage surface[19], which can be used to predict the potential failure surface of the slope. The generalized Hoek-Brown criterion is expressed in the form

$$\sigma_1-\sigma_3=\sigma_{ci}\left(m_b\frac{\sigma_3}{\sigma_{ci}}+s\right)^a \tag{1}$$

where σ_1 is the maximum principal stress at the time of rock failure (pressure as positive); σ_3 is the minimum principal stress; σ_{ci} is the uniaxial compressive strength of the intact rock; m_b, s and a are constants that reflect the rock mass and rock type, which can be determined by the following equation

$$m_b=m_i\cdot\exp\left(\frac{\mathrm{GSI}-100}{28-14D}\right) \tag{2}$$

$$s=\exp\left(\frac{\mathrm{GSI}-100}{9-3D}\right) \tag{3}$$

$$a=\frac{1}{2}+\frac{1}{6}\left[\exp\left(-\frac{\mathrm{GSI}}{15}\right)-\exp\left(-\frac{20}{3}\right)\right] \tag{4}$$

where D is the disturbance coefficient, whose value ranges from 0 to 1, which is related to the excavation method and the degree of disturbance of the rock mass; GSI is the geological strength index. The deformation modulus and Poisson's ratio of the rock mass can be obtained from the following equation[20]:

$$E_m=\left(1-\frac{D}{2}\right)\sqrt{\frac{\sigma_{ci}}{100}}\cdot10^{((\mathrm{GSI}-10)/40)} \tag{5}$$

$$v=-0.002\mathrm{GSI}-0.003m_i+0.457 \tag{6}$$

where E_m is the deformation modulus (GPa) of the rock mass; and v is the Poisson's ratio.

2.2 Random Field Theory

Vanmarck[21] proposed random field theory to describe the spatial variability of geotechnical parameters. In random field theory, the mean value, coefficient of variation, correlation coefficient and scale of fluctuation of parameters are the key parameters describing the spatial autocorrelation of rock mass. In the process of generating random field generation of geotechnical material parameters, it is generally assumed that the parameters obey lognormal distribution. Because the lognormal distribution can effectively avoid generating negative parameter values. Numerous geological investigations and applications have demonstrated that the lognormal distribution can well describe the spatial variability of geotechnical material parameters[22–23]. If a parameter obeys a lognormal distribution, and the mean value μ_{ln} and variance σ_{ln}^2 are logarithm then the relationship between the logarithm of the parameter and the mean and variance of the parameter itself is

$$\mu=\exp\left(\mu_{ln}+\frac{\sigma_{ln}^2}{2}\right) \tag{7}$$

$$\sigma^2=[\exp(\sigma_{ln}^2)-1]\exp(2\mu_{ln}+\sigma_{ln}^2) \tag{8}$$

where μ and σ^2 are the mean and variance of the parameter; μ_{ln} and σ_{ln}^2 are the mean and variance of the logarithm of the parameter. In addition to the mean and variance in the distribution function, the autocorrelation function is used to describe the autocorrelation of a single parameter in space. For example, in a two-dimensional space, it is assumed that the autocorrelation function of the parameters is

$$\rho(\tau_x,\tau_y)=\exp\left[-\left(\frac{2\tau_x}{\delta_h}+\frac{2\tau_y}{\delta_v}\right)\right] \tag{9}$$

where ρ is the autocorrelation coefficient between two points; τ_x and τ_y are the horizontal and vertical

distances between meshes; δ_{h} and δ_{v} are the horizontal and vertical scale of fluctuation. There are also many methods to generate random fields, such as local averaging method, K-L expansion method, and Cholesky decomposition method. Since the Cholesky decomposition method has the advantages of simple calculation and easy implementation of the program, this paper uses the Cholesky decomposition method to generate random fields:

$$\boldsymbol{L}\times\boldsymbol{L}^{\mathrm{T}}=\boldsymbol{C} \tag{10}$$

$$\boldsymbol{C}=\begin{bmatrix} 1 & \rho(\tau_{x_{1,2}},\tau_{y_{1,2}}) & \cdots & \rho(\tau_{x_{1,n}},\tau_{y_{1,n}}) \\ \rho(\tau_{x_{2,1}},\tau_{y_{2,1}}) & 1 & \cdots & \rho(\tau_{x_{2,n}},\tau_{y_{2,n}}) \\ \vdots & \vdots & \ddots & \vdots \\ \rho(\tau_{x_{n,1}},\tau_{y_{n,1}}) & \rho(\tau_{x_{n,2}},\tau_{y_{n,2}}) & \vdots & 1 \end{bmatrix} \tag{11}$$

where C is the correlation matrix, where n is the total number of meshes; $\boldsymbol{L}$ is the matrix obtained by Cholesky decomposition, and generates the correlation standard normal random field G_i under the given matrix conditions

$$G_i=\sum_{k=1}^{i}\boldsymbol{L_{ik}}\boldsymbol{Z_k}\quad i=1,2,\cdots\cdots,n \tag{12}$$

where $\boldsymbol{Z_k}$ are independent standard normal random variables.

2.3 Failure probability calculation

The strength reduction method has been widely used due to its practicality and reliability. The principle of this method is to change the value of the geotechnical strength parameters by varying the reduction coefficient until the slope becomes unstable. The strength reduction based on the Mohr-Coulomb criterion is shown as follows:

$$\tan\varphi_{\mathrm{t}}=\frac{\tan\varphi}{F} \tag{13}$$

$$c_{\mathrm{t}}=\frac{c}{F} \tag{14}$$

where φ and c are the friction angle and cohesion before reduction; φ_{t} and c_{t} are the friction angle and cohesion after reduction; and F is the discount factor. With the continuous decrease of cohesive force and internal friction angle, the slope gradually is destabilized, and the calculation does not converge at the same time. However, the strength reduction method based on the Hoek-Brown criterion needs to be converted to the Mohr-Coulomb criterion first, and then the slope safety factor is determined by reducing the instantaneous friction angle and cohesion force[24]:

$$\tau=\sigma'\tan\varphi_{\mathrm{c}}+c_{\mathrm{c}} \tag{15}$$

where τ and σ' are the shear stress and normal stress; φ_{c} and c_{c} are the instantaneous friction angle and cohesion, which can be calculated by the following equation:

$$\varphi_{\mathrm{c}}=2\tan^{-1}\sqrt{N_{\varphi_{\mathrm{c}}}}-90^{\circ} \tag{16}$$

$$c_{\mathrm{c}}=\frac{\sigma_{\mathrm{c}}^{\mathrm{ucs}}}{2\sqrt{N_{\varphi_{\mathrm{c}}}}} \tag{17}$$

where $N_{\varphi_{\mathrm{c}}}$ and $\sigma_{\mathrm{c}}^{\mathrm{ucs}}$ are the calculated intermediate quantities, which are deduced from the minimum principal stress σ_3 and other parameters:

$$N_{\varphi_{\mathrm{c}}}=1+am_{\mathrm{b}}\left(m_{\mathrm{b}}\frac{\sigma_3}{\sigma_{\mathrm{ci}}}+s\right)^{a-1} \tag{18}$$

$$\sigma_{\mathrm{c}}^{\mathrm{ucs}}=\sigma_3(1-N_{\varphi_{\mathrm{c}}})+\sigma_{\mathrm{ci}}\left(m_{\mathrm{b}}\frac{\sigma_3}{\sigma_{\mathrm{ci}}}+s\right)^{a} \tag{19}$$

In this paper, Monte Carlo simulation method is used to evaluate the failure probability of engineering cases. It inputs a large number of random variables $\boldsymbol{X}$ into the analysis model and then probability of occurrence of the event is analyzed after calculation. The failure probability P_{f} is defined as follows:

$$P_{\mathrm{f}}=\frac{1}{N_{\mathrm{MC}}}\sum_{i=1}^{N_{\mathrm{MC}}}I[\mathrm{FS}_i(\hat{\boldsymbol{X}}_i)<1] \tag{20}$$

$$I=\begin{cases}0, & \text{if } \mathrm{FS}_i\geqslant 1\\ 1, & \text{if } \mathrm{FS}_i<1\end{cases} \tag{21}$$

where N_{MC} is the number of Monte Carlo simulations; FS_i is the safety factor calculated for the ith time; and I is an indicative function.

As shown in Eq. (20), the failure probability P_{f} is related to the number of Monte Carlo simulations. Therefore, the convergence analysis is necessary to calculate the failure probability using Monte Carlo simulation method. As the number of Monte Carlo simulations increases, the failure probability will gradually converge to a constant value. When the coefficient of variation of the failure probability is less than a certain value, the failure probability at this time is the failure probability of the slope. In this paper, the coefficient of variation $\mathrm{COV}_{P_{\mathrm{f}}}$ of the failure probability will be determined according to Eq. (22). It is judged that the calculation is converged when $\mathrm{COV}_{P_{\mathrm{f}}}$ is less than 0.3[25]. In order to verify the reasonableness of the number of simulations further, the variation of the mean and standard deviation of the safety factor with the number of simulations will be analyzed.

$$\mathrm{COV}_{P_{\mathrm{f}}}=\sqrt{(1-P_{\mathrm{f}})/(N_{\mathrm{MC}}\cdot P_{\mathrm{f}})} \tag{22}$$

3 Numerical model and working conditions

3.1 Model validation

The example of homogeneous slope[26] is employed to verify the feasibility of the proposed method. The slope calculation model and mesh division are shown in Fig.1. The slope height is 10 m and the slope angle is 45°. In order to meet the calculation accuracy requirements, the meshes are quadrilaterals and triangles

with a side length of 0.5 m[27]. The rock mass parameters are shown in Table 1, and the safety factor calculated[26] using the strength reduction method based on finite elements is 1.15. While the safety factor calculated in this paper based on the strength reduction method in FlAC^{3D} for simulation analysis is 1.176. The safety factors calculated by both are close to each other, which indicates that the model calculation method is applicable. The slight difference between them may be due to the difference of model meshing and the different calculation methods of finite element method and finite difference method.

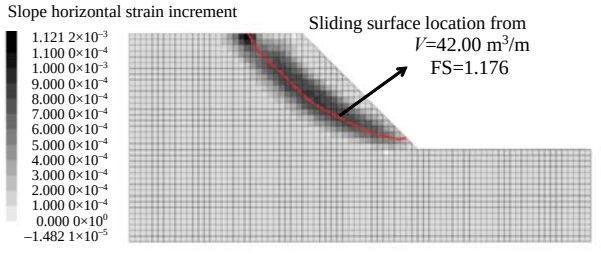

Fig. 1 Analysis results of slope model and stability

3.2 Introduction of working conditions

Mayer et al.[28] statistically analyzed the geological strength index and uniaxial compressive strength of different rock masses in the region and found that the correlation length of spatial variation varied from tens to hundreds of meters. Öztürk et al.[29] used the ReV technique to study the spatial variation of uniaxial compressive strength σ_{ci}, Rock Quality Designation (RQD), Schmidt hardness and static cutting rate of rock masses. Mao et al.[30] treated GSI, m_i, σ_{ci} and D as random variables to study the ultimate bearing capacity of strip foundation. In order to examine the influence of spatial variability of rock strength parameters on the probability of slope failure, simulation analysis conditions with different random field description parameters are set up on the basis of deterministic analysis. In this paper, the geological strength index (GSI) is considered as a random variable, while the uniaxial compressive strength σ_{ci} and the material constant for the intact rock m_i are considered as random field variables. All three variables obey lognormal distribution[20, 31–32]. For GSI , Ching et al.[33] noted that this parameter was judged by engineering tests, which characterize the overall condition of the rock mass and do not represent the spatial variation of the precise physical parameters. For the correlation between σ_{ci} and m_i, the literature[34] states that the correlation coefficient varies from –0.242 38 (sandstone) to –0.79432(marble). According to the relevant literature, different working conditions are selected for simulation. The input parameters are shown in Table 2, where GSI as a random variable. Its coefficient of variation is taken as the same value as the coefficient of variation of the random field.

Table 1 Properties of the rock slope

Elastic modulus E /MPa	Poisson's ratio ν	Unit weight γ /(MN·m^{-3})	Uniaxial compressive strength σ_{ci} /MPa	Geological strength Index GSI	Material constant for the intact rock m_i	Perturbation factor D	m_b	s	a
5 000	0.3	0.025	30	5	2	0	0.067	2.5×10^{-5}	0.169

Table 2 Rock mass parameters of random field model

Parameters	Mean value	Coefficient of variation	Scale of fluctuation	Correlation coefficient
Geological Strength Index GSI	5	0.1–0.5	—	—
Material constant for the intact rock m_i	2	0.1–0.5	δ_h = 2, 6, 10, 25, 50, 75, 100 m	$\rho_{m_i,\sigma_{ci}}$ = –0.7– –0.3
Uniaxial compressive strength σ_{ci}	30	0.1–0.5	δ_v = 2, 6, 10, 25, 50, 75, 100 m	$\rho_{m_i,\sigma_{ci}}$ = –0.7– –0.3

4 RFDM-based slope failure probability calculation process

In order to understand the calculation method of slope failure probability considering the spatial variability of rock strength parameters proposed in this paper, the failure probability calculation process is illustrated by Fig.2. The process is divided into six steps.

Firstly, the geological and geometric parameters of the slope are determined, and then the uncertainties of the parameters are described by mean value, coefficient of variation and autocorrelation function.

Generate N_{MC} random samples by Latin hypercube sampling.

Use the Fish language in FLAC^{3D} to construct functions and to obtain the center coordinates of each mesh, and then generate the corresponding correlation matrix $\boldsymbol{C}$ based on the autocorrelation function of Eq.(9) through the relationship between the coordinates of the meshes.

The Cholesky decomposition of the correlation matrix $\boldsymbol{C}$ yields the triangular matrix $\boldsymbol{L}$, and obtain the lognormal random field.

Calculate the safety factor of each slope and calculate the failure probability P_f by Monte Carlo simulation method according to Eqs. (20) and (21).

Calculate the COV_{P_f} for the slope failure probability P_f. If the COV_{P_f} is less than 0.3, then P_f is the slope failure probability. Otherwise, it is necessary to increase the number of Monte Carlo simulations and repeat steps (2) to (5) until it is less than 0.3.

5 Slope reliability analysis

In this section, the effect of different random field description parameters (coefficient of variation COV, scale of fluctuation δ and correlation coefficient ρ)

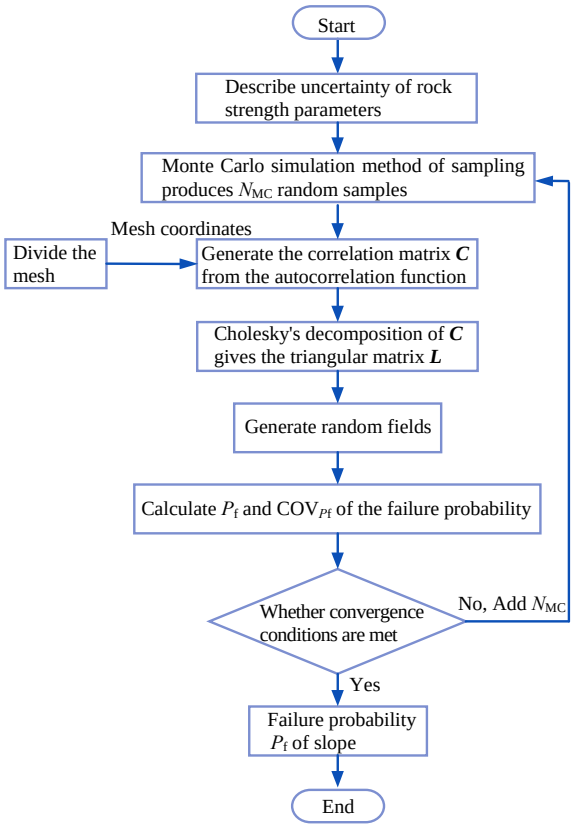

Fig. 2 Flow chart of calculation

on the slope failure probability and slip volume is investigated for the slope without an anti-slide pile. In order to improve the computational efficiency and ensure the accuracy of the failure probability, different numbers of Monte Carlo simulations are analyzed. Figure 3(a) shows the gradual convergence of the mean and standard deviation of the slope safety factor with the number of simulations. It is calculated that when the number of simulations is 1,000 times, $\mathrm{COV}_{P_f} < 0.3$, which meets the calculation accuracy requirement. Therefore, the distribution of the slope factor of safety obtained from the random field model is fitted as shown in Fig.3(b) when the Monte Carlo simulation is performed 1000 times.

Since the range of slope instability is closely related to the slip volume, this paper uses the slope slip volume to make a simple assessment of the range of slope instability. Firstly, the displacement field at the end of the calculation for each model of FLAC^{3D} is exported. Since there is a difference between the displacement of the slope slip area and the stable area, the cluster analysis algorithm in Matlab can be used to automatically classify the slip area and the stable area according to the displacement size, and the coordinate points corresponding to the slip area are also distinguished. Then the coordinate points of the slip area are derived and the area of the slip area is calculated, which is the slip area of the two-dimensional slope instability. The predicted horizontal strain increment and slip area of the homogeneous slope are shown in Fig. 1, which are in agreement with the numerical simulation results. This shows that the method is reliable.

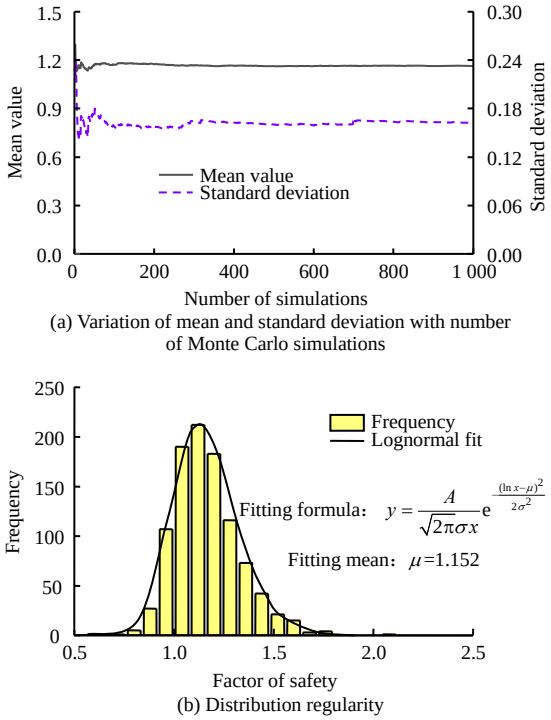

(a) Variation of mean and standard deviation with number of Monte Carlo simulations

(b) Distribution regularity

Fig. 3 Convergence and distribution of safety of factor

5.1 Effect of coefficient of variation

Figure 4 shows the effect of the coefficient of variation on the probability of slope failure and slip volume. The correlation coefficient $\rho_{m_i,\sigma_{ci}} = -0.3$, the horizontal scale of fluctuation $\delta_h = 10$ m, and the vertical scale of fluctuation $\delta_v = 6$ m. As can be seen from the figure, both the failure probability and the slip volume increase significantly with COV increasing. The probability of failure is close to 0 when COV = 0.1, while the probability of failure is 37.03% at COV = 0.5, which is a large difference between the two. This shows the great influence of the coefficient of variation of rock parameters on the reliability of slopes. Therefore, in practical engineering, the slope rock masses with large variability should be given sufficient attention. Figure 4(b) shows the probability density function curve after fitting the factor of safety obtained from the Monte Carlo simulation. The curve pattern progresses from tall and lean to short and fat with the increase of COV and a gradual leftward shift of the mean value. This leads to an increase in the area of factor of safety less than 1 in the probability density curve and an increase in the probability of failure.

5.2 Effect of correlation coefficient

In order to explore the influence of the intercorrelation between uniaxial compressive strength σ_{ci} and material constant for the intact rock m_i on slope reliability, the variation range of $\rho_{m_i,\sigma_{ci}}$ is taken from –0.7 to –0.3, the coefficient of variation is taken to be 0.3, $\delta_h = 10$ m and $\delta_v = 6$ m. Figure 5(a) gives the variation curves of slope failure probability over slip volume with $\rho_{m_i,\sigma_{ci}}$. It is found that the slope failure probability and slip volume increase generally with increasing

$\rho_{m_i,\sigma_{ci}}$. After fitting a lognormal distribution to the factor of safety, the slope failure probability increases from 10.8% to 15.5% when $\rho_{m_i,\sigma_{ci}}$ increases from –0.7 to –0.3, the mean value for the factor of safety decreases from 1.159 to 1.149 and the standard deviation increases from 0.13 to 0.16. This results in Fig. 5(b) where the probability density function curve becomes short and fat and the peak is left-skewed. It can be seen that the correlation coefficient has a large influence on the slope reliability, and the stability of the slope is favored when the rock parameters have a strong negative correlation.

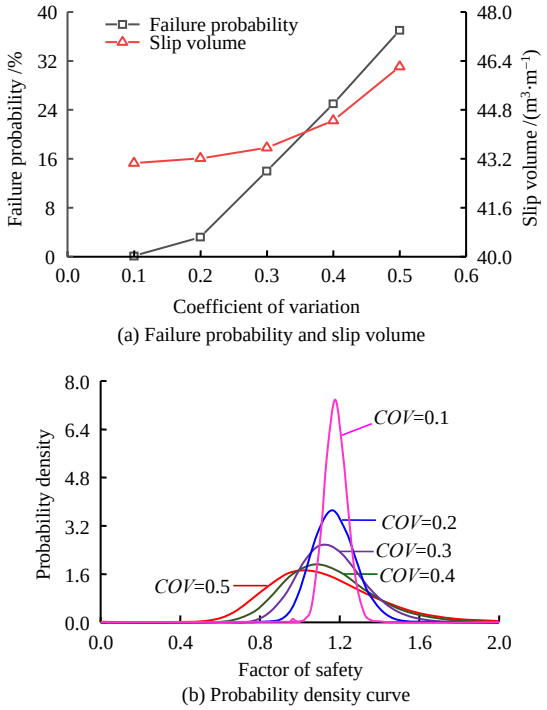

Fig. 4 Influences of different COVs on failure probability of slope and volume of slip mass

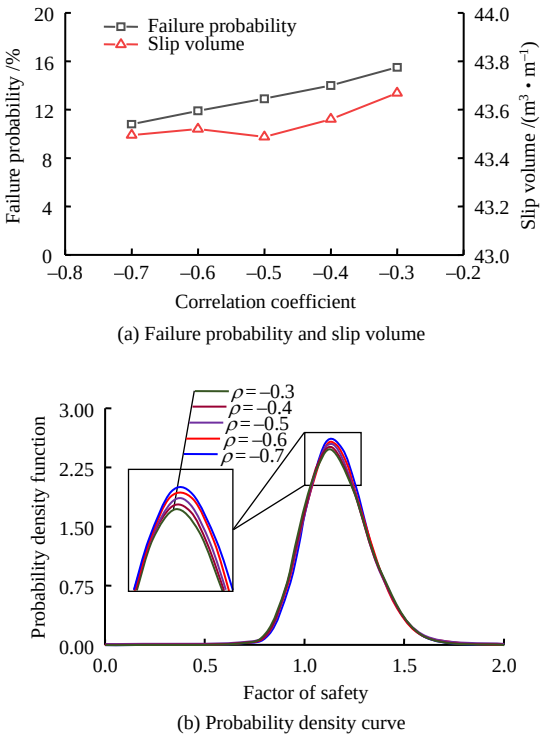

Fig. 5 Influences of different $\rho_{m_i,\sigma_{ci}}$ on failure probability of slope and volume of slip mass

5.3 Effect of fluctuation scale

In order to examine the effect of the scale of fluctuation on slope reliability, Figure 6 compares the effect of different horizontal scale of fluctuation δ_h and vertical scale of fluctuation δ_v on slope failure probability and slip volume. It is assumed that COV is 0.3 and $\rho_{m_i,\sigma_{ci}}$ is –0.4. To analyze the effect of δ_h, δ_v is set to be 10 m and the variation range of δ_h is from 2 to 100 m. Conversely, to study the effect of δ_v, δ_h is set as 10 m and the variation range of δ_v is from 2 to 100 m. As shown in Fig. 6(a), the failure probability increases with δ_h, and the trend of δ_v increases and then decreases, and the influence of δ_h on the slope failure probability is greater than the influence of δ_v on the slope failure probability. The trend of failure probability and slip volume variation is obvious when the scale of fluctuation is within 2 to 10 m. However, as the scale of fluctuation increases the variability of failure probability decreases. The stronger the spatial correlation of rock parameters, the weaker the variability, and the smaller the fluctuation of damage probability and slip variation. It is worth noting that when $\delta_v = 75$ m, the probability of failure is reduced compared with that at $\delta_v = 50$ m. At this time, the rock mass in the vertical direction is more homogeneous, which further slows down the slope instability. When $\delta_h > 25$ m, the slip volume is still decreasing gradually. However, when δ_v exceeds 25 m, the slip volume increases slightly.

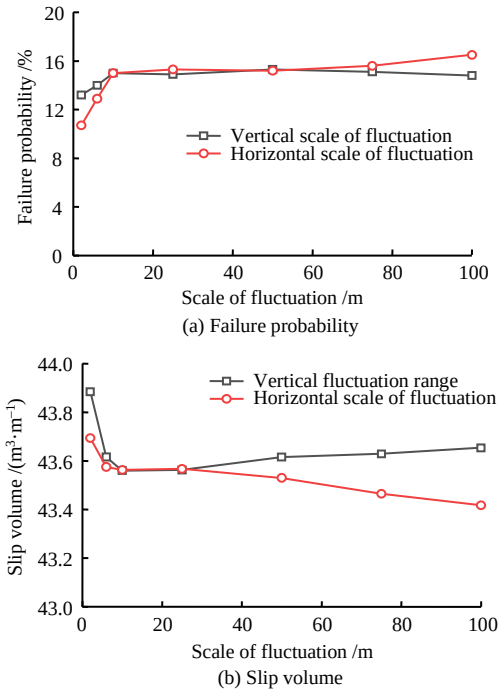

Fig. 6 Influences of different δ on failure probability of slope and volume of slip mass

This may be because when δ_v increases with δ_h constant, the variability of rock parameters in the horizontal direction remains the same, while the vertical rock parameters tend to be more homogeneous. It can reduce the influence brought by the weak zone of rock mass, which is beneficial to slope stability. However, it makes the slip surface in slope change and the slip volume increase.

5.4 Comparison of slip modes

To further compare the differences in shape and location of the critical slip surfaces of the slopes obtained from different random field models, the typical critical slip surfaces of the slopes and their corresponding sample cloud atlas of rock strength parameters for the three random field models are selected in Fig. 7. Figure 7(a) shows the shallow slip mode located on the slope surface. Figure 7(c) shows the deep slip pattern located at the toe of the slope. And the landslide shear outlet in Fig. 7(b) is located at the toe of the slope. The shape of the slip surface is similar for these three modes, and all of them show a downward concave shape. Although the uniaxial compressive strength of the slope in Fig. 7(a) is smaller overall, its distribution is more uniform and the safety factor is closer to that of the homogeneous slope. However, although the local rock strength in the slope in Fig. 7(c) is larger, its slip surface still passes through the area with weaker rock parameters, resulting in a smaller factor of safety. The differences in the factor of safety for the above three typical samples and their landslide locations and shapes indicate that the spatial variability of rock parameters significantly affects the slope factor of safety with respect to slip surface locations, shapes and slip volumes for the specified slopes, which are very different from the results of the deterministic analysis.

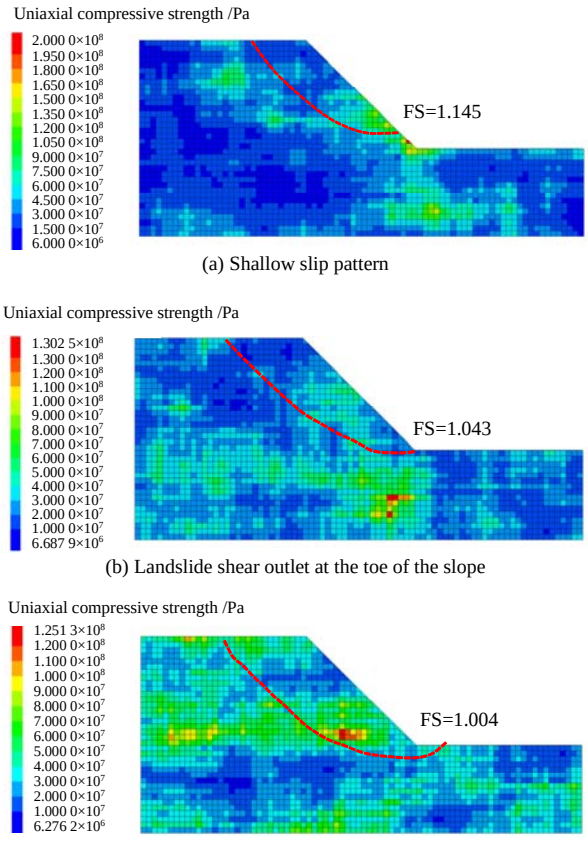

(a) Shallow slip pattern

(b) Landslide shear outlet at the toe of the slope

(c) Deep slip mode

Fig. 7 Typical samples and analysis results of random fields

6 Pile response and slope reliability

It can be seen from the analysis in Chapter 5 that the spatial variability of rock mass will affect the reliability of slope. In order to reduce the loss caused by slope instability, anti-slide piles are commonly used to support the slope. In this chapter, the same simulation scheme as in Chapter 5 will be used to study the slope supported by anti-slide piles. Firstly, deterministic analysis was performed with different pile lengths and pile positions for five points as shown in Fig. 8(a). The anti-slide pile treatment method was referred to the literature[35], and structural unit piles with a modulus of elasticity of 34GPa and Poisson's ratio of 0.15 were used. The results shown in Fig. 8(b) indicate that the slope factor of safety is the highest when the anti-slide pile is located at point *C* and the pile length is 19 m. The horizontal strain cloud atlas of the slope is shown in Fig. 8(a), and the following studies are carried out based on this condition.

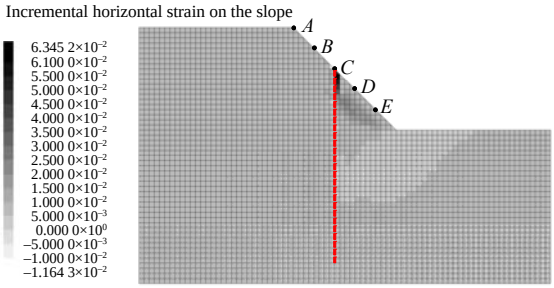

(a) Distribution of piles

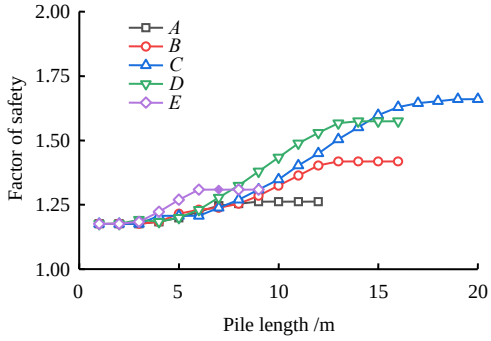

(b) Change in factor of safety

Fig. 8 Influence of different pile locations and pile lengths on slope stability

The maximum displacement and maximum bending moment at the top of the pile for the laterally loaded piles are important parameters for designing piles[36]. As a kind of laterally loaded pile, the anti-slide pile is difficult to express explicit expressions due to its maximum bending moment and displacement solution.

Therefore, its statistical properties such as mean and standard deviation are difficult to obtain. A large number of calculations are needed to determine the statistical properties. In this section, we will study the response of anti-slide piles considering the spatial variability of rock mass and the estimation of slope failure probability. In order to improve the computational efficiency and meet the accuracy requirements, it can be found from Fig.9 that the mean and standard deviation of the pile top displacement and maximum bending moment converge when the number of simulations is 500, and the scale of fluctuation is less than 5%[36].

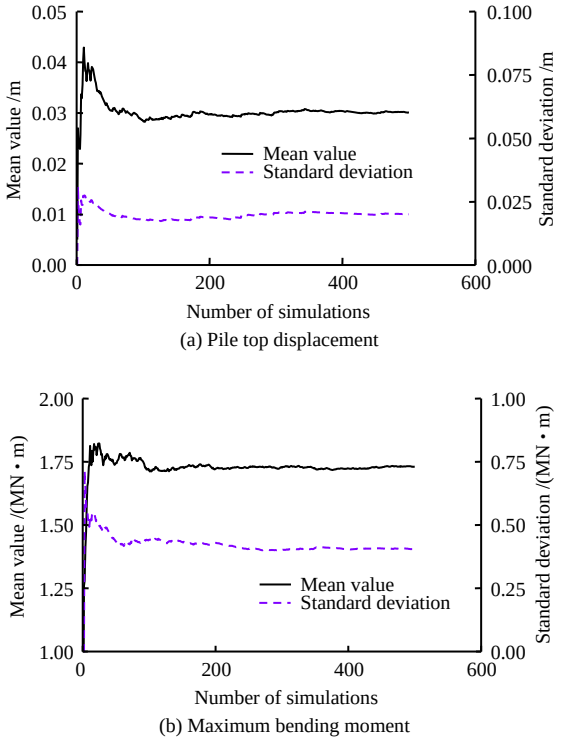

Fig. 9 Variations of mean and standard deviation of monitoring parameters with the number of simulations

6.1 Effect of coefficient of variation

The effect of spatial variability on the horizontal bearing capacity and maximum bending moment of laterally loaded piles was studied[36]. It is found that the horizontal load and pile top displacement show a positive correlation, and the law of variation of the mean value of maximum bending moment is similar to that of the mean value of bearing capacity. These regulations provide a reference for the research in this section. Fig.10 depicts the variation of mean value and coefficient of variation of displacement of anti-slide pile and maximum bending moment of anti-slide pile top under different coefficients of variation.

From section 5.1, it can be seen that as the coefficient of variation of rock mass increases, the slope failure probability and slip volume increase, the slip force increases and the instability is enhanced. This may make the bearing capacity of the anti-slide pile decrease, which leads to an increase in the mean value of pile top displacement and a decrease in the mean value of maximum bending moment. While the coefficient of variation of the maximum bending moment has the opposite trend, which is unfavorable for the design and construction of pile foundation. Therefore, sufficient attention should be paid to the rock variability in practical engineering.

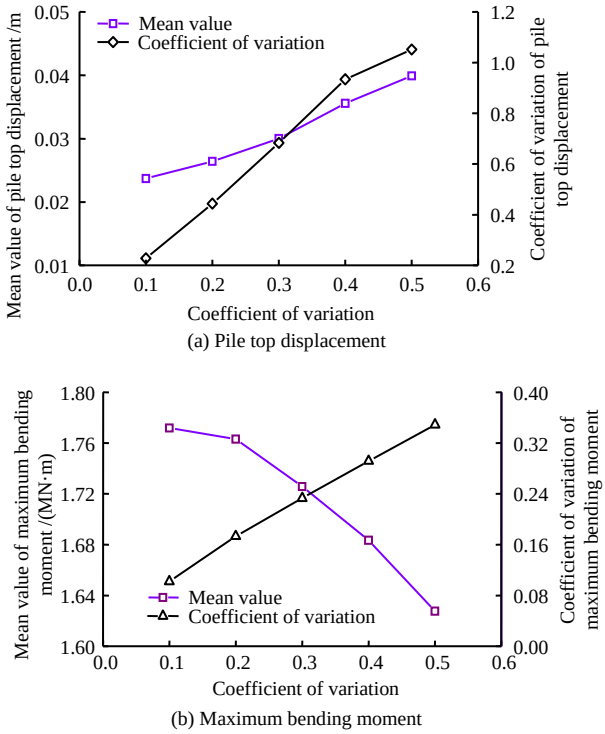

Fig. 10 Influence of different COV on monitoring parameters of anti-sliding pile

6.2 Effect of correlation coefficient

The effect of correlation coefficient $\rho_{m_i,\sigma_{ci}}$ change on the pile random response is given in Fig. 11. From the analysis in section 5.2, it can be seen that as the correlation coefficient increases, the negative correlation between the rock parameters decreases and the slope failure probability and slip volume increase. This may lead to an increase in the sliding force of the slope, an increase in the mean value of the pile top displacement and a decrease in the mean value of the maximum bending moment. However, it can be observed from Fig. 11 that the correlation coefficient of rock has a significant effect on the coefficient of variation of pile top displacement than on the coefficient of variation of maximum bending moment. This indicates a high degree of dispersion of pile top displacement. In order to avoid losses, the variability of the rock mass needs to be fully considered in the design to reduce the variability of the pile top displacement caused by the rock mass variability. The mean value and standard deviation of maximum bending moment have the same trend as in section 5.1. The mean value decreases while the coefficient of variation is increasing, but the range of variation is small.

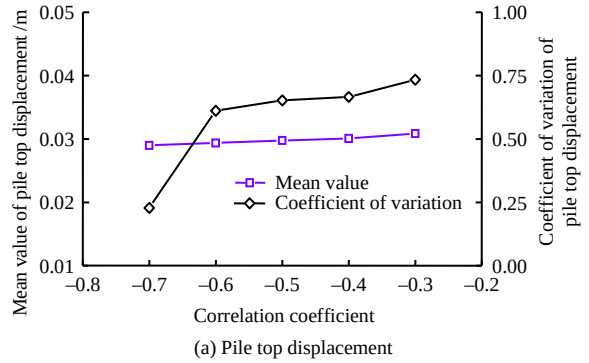

(a) Pile top displacement

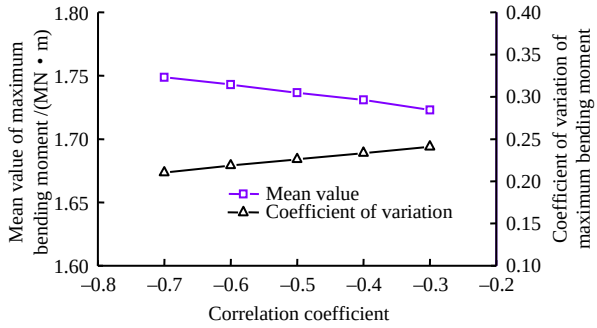

(b) Maximum bending moment

Fig. 11 Influence of different $\rho_{m_i,\sigma_{ci}}$ on monitoring parameters of anti-sliding pile

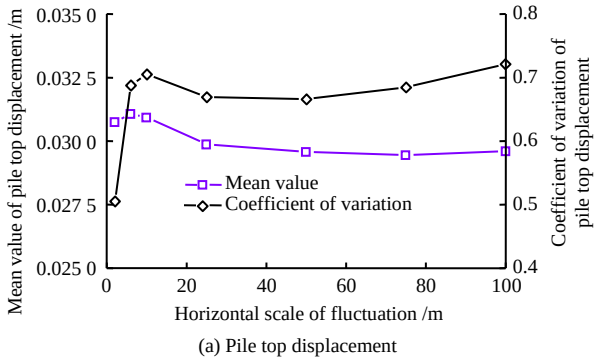

(a) Pile top displacement

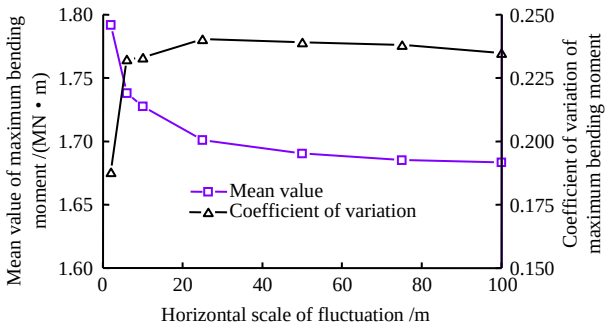

(b) Maximum bending moment

Fig. 12 Influences of different δ_h on monitoring parameters of anti-sliding pile

6.3 Effect of fluctuation scale

Figures 12 and 13 compare the effects of different fluctuation ranges on the displacement and maximum bending moment at the top of the anti-slide pile. From the figures, it can be observed that with the increase of fluctuation range, the mean value of pile top displacement has a trend of increasing and then decreasing. While the mean value of maximum bending moment is continuously decreasing, its coefficient of variation changes in the opposite direction. This phenomenon is not conducive to the stability of the pile. When the fluctuation range is less than 25 m, the mean values of pile top displacement and maximum bending moment change significantly. The mean value of pile top displacement reaches the maximum δ_v at 25 m. This may be due to the fact that 25m is close to the fluctuation range of the "worst case" of the slope[36]. From the analysis in section 5.3, it can be seen that when the fluctuation range is larger, the overall probability of failure is also increasing. However, the slip volume has a tendency to decrease. It can be found that the increase of scale of fluctuation of rock parameters may reduce the influence range of slope instability, and thus the mean value of pile top displacement decreases. The degree to which the pile random response is affected by the scale of fluctuation is also decreasing. The analysis shows that the effect of δ_v on pile response is less than the effect of δ_h, because the increase of δ_v makes the rock mass in the vertical direction of the slope tend to be homogeneous and can resist the slip together with the anti-slide pile.

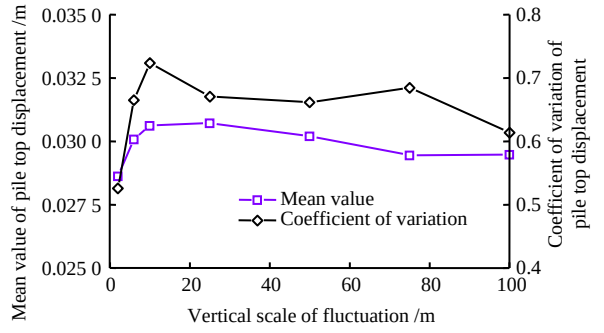

(a) Pile top displacement

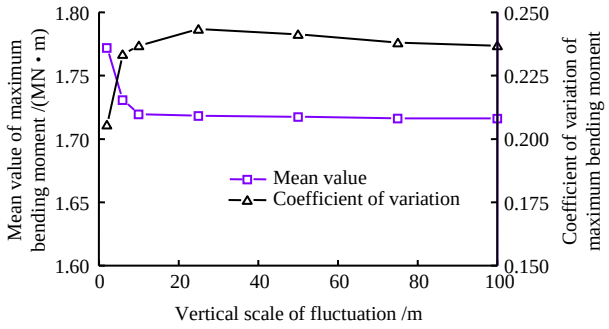

(b) Maximum bending moment

Fig. 13 Influences of different δ_v on monitoring parameters of anti-sliding pile

6.4 Estimation of slope failure probability

Since the failure probability of the reinforced slope is very small, tens of thousands of calculations are required to obtain a more accurate slope failure probability using Monte Carlo simulations[15]. Therefore, in order to

obtain more accurate slope failure probabilities while improving the computational efficiency, the safety factor obtained from Monte Carlo simulations can be fitted to the distribution to estimate the failure probability of the anti-slide pile reinforced slope[37]. Firstly, the failure probability obtained from the Monte Carlo simulation of the unreinforced slope was compared with the failure probability obtained after fitting the safety factor with lognormal distribution, as shown in Fig.14. It is found that there is an error between the two, but it is within 20% and the coefficient of determination $R^2 = 0.987$. It shows that the fitting result meets the requirement of calculation accuracy. Therefore, the failure probability can be estimated by the lognormal method. After 500 Monte Carlo simulations, the factor of safety of the anti-slide pile reinforced slope considering the spatial variability of the rock mass also approximately obeys the lognormal distribution, and its mean and standard deviation have stabilized. Therefore, the probability of failure is estimated after fitting the lognormal distribution to the factor of safety, as shown in Fig. 15.

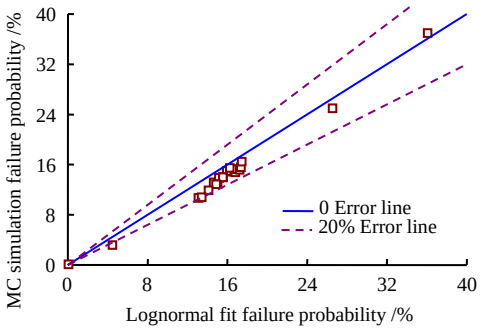

Fig. 14 Comparison of failure probability of unreinforced slopes

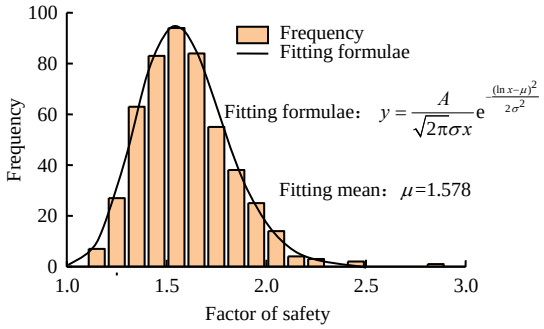

Fig. 15 Fitting of safety of factor

Figure 16 shows the effect of different random field description parameters on the failure probability of the anti-slide pile reinforced slope. It can be seen from the figure that the failure probability increases with the increase of COV , $\rho_{m_i,\sigma_{ci}}$ and δ , where COV has the greatest impact on the failure probability, and the effect of δ_v on the slope failure probability is smaller than the effect of δ_h on the failure probability.

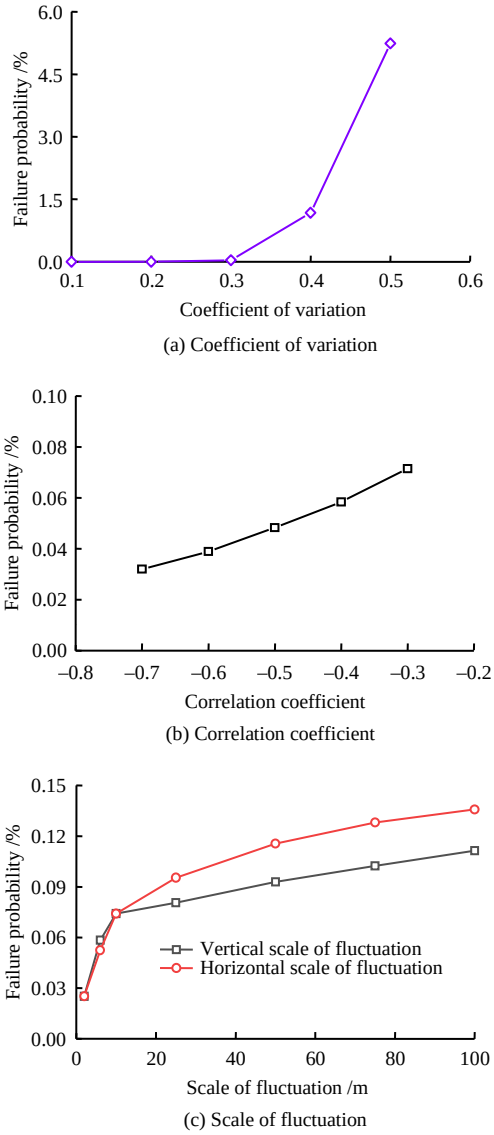

Fig. 16 Influences of different random field description parameters on failure probability of slope reinforced by anti-slide piles

7 Conclusions

(1) The coefficient of variation, correlation coefficient and scale of fluctuation of rock strength parameters have obvious influence on the reliability of the slope system. When the variability of rock parameters or the negative correlation between rock parameters is large, ignoring the spatial variability of parameters will obviously overestimate the failure probability of unreinforced slopes. The failure probability increases with δ_h increase, and tends to increase and then decrease with δ_v increase.

(2) Through Monte Carlo simulation of the anti-slide pile reinforced slope and statistical analysis of the pile top displacement and maximum bending moment, it was found that the spatial variability of the rock mass had a significant effect on the random response of the pile. The mean value and coefficient of variation of pile top displacement showed the same trend with different random field description parameters. The mean value of maximum bending moment decreased

with the increase of COV, $\rho_{m_i,\sigma_{ci}}$ and δ, but its coefficient of variation increased. The pile top displacement in the deterministic analysis is 0.010 5 m, which is higher than this value for all the working conditions in the random field analysis. The maximum bending moment is 1.8 MN • m, while it is lower than this value for all conditions in the random airport analysis. This indicates that neglecting the spatial variability of the rock mass will have a negative impact on the optimal design of the anti-slide pile compared with the deterministic analysis.

(3) Monte Carlo simulations were performed on the slopes strengthened by anti-slide piles, and the factor of safety obtained from the simulations was fitted to the lognormal distribution to estimate the failure probability of the slopes reinforced by anti-slide piles. It is found that the failure probability increases with the increase of COV and δ for the slopes reinforced by anti-slide piles. The effect of COV on the failure probability is the largest, and the effect of δ_v on the slope failure probability is smaller than the effect of δ_h on the failure probability.

In this paper, slope reliability analysis and pile random response considering the spatial variability of rock parameters are studied, and the geological strength index GSI is considered as an index to evaluate the quality of rock masses. However, for the rock mass whose damage is mainly controlled by the structural surface, the application of random field needs further study.

References

[1] CHEN L, ZHANG W, GAO X, et al. Design charts for reliability assessment of rock bedding slopes stability against bi-planar sliding: SRLEM and BPNN approaches[J]. Georisk: Assessment and Management of Risk for Engineered Systems and Geohazards, 2020: 1–16.

[2] CHEN L, ZHANG W, ZHENG Y, et al. Stability analysis and design charts for over-dip rock slope against bi-planar sliding[J]. Engineering Geology, 2020, 275: 105732.

[3] OGUZ E A, YALCIN Y, HUVAJ N. Probabilistic slope stability analyses: effects of the coefficient of variation and the cross-correlation of shear strength parameters[M]// Geotechnical Frontiers 2017, 2017: 363–371.

[4] ZHANG R, GOH A T C, LI Y, et al. Assessment of apparent earth pressure for braced excavations in anisotropic clay[J]. Acta Geotechnica, 2021, 16(5): 1615–1626.

[5] LI Y, ZHANG W. Investigation on passive pile responses subject to adjacent tunnelling in anisotropic clay[J]. Computers and Geotechnics, 2020, 127(3): 103782.

[6] TANG Hong-xiang, WEI Wen-cheng. Finite element analysis of slope stability by coupling of strength anisotropy and strain softening of soil[J]. Rock and Soil Mechanics, 2019, 40(10): 4092–4100.

[7] XUE Yang, WU Yi-ping, MIAO Fa-sheng, et al. Seepage and deformation analysis of Baishuihe landslide considering spatial variability of saturated hydraulic conductivity under reservoir water level fluctuation[J]. Rock and Soil Mechanics, 2020, 41(5): 1709–1720.

[8] HUANG D, SONG Y X, MA G W, et al. Numerical modeling of the 2008 Wenchuan earthquake-triggered Niumiangou landslide considering effects of pore-water pressure[J]. Bulletin of Engineering Geology and the Environment, 2019, 78(7): 4713–4729.

[9] WANG Chuan, LENG Xian-lun, LI Hai-lu, et al. Probabilistic stability analysis of underground caverns considering spatial variation of joint distribution[J]. Rock and Soil Mechanics, 2021, 42(1): 224–233.

[10] LI Jing-ping, CHENG Yong-gang, LI Dian-qing, et al. System reliability analysis of spatially variable soil slopes using the multiple response surfaces method[J]. Rock and Soil Mechanics, 2016, 37(1): 147-155, 165.

[11] JIANG Shui-hua, LI Dian-qing, ZHOU Chuang-bing et al. Slope reliability analysis considering effect of autocorrelation functions[J]. Chinese Journal of Geotechnical Engineering, 2014, 36(3): 508–518.

[12] CHENG H, CHEN J, CHEN R, et al. Risk assessment of slope failure considering the variability in soil properties[J]. Computers and Geotechnics, 2018, 103(11): 61–72.

[13] HUANG Jun, ZHAO Jiang, DUAN Xiang-rui, et al. Reliability analysis for soil slopes reinforced with piles using shear strength reduction method[J]. Journal of Civil and Environmental Engineering, 2020, 42(6): 11–18.

[14] TEIXEIRA A, HONJO Y, CORREIA A G, et al. Sensitivity analysis of vertically loaded pile reliability[J]. Soils and Foundations, 2012, 52(6): 1118–1129.

[15] Chen F, Zhang R, Wang Y, et al. Probabilistic stability analyses of slope reinforced with piles in spatially variable soils[J]. International Journal of Approximate Reasoning, 2020, 122: 66–79.

[16] GONG W, TANG H, JUANG C H, et al. Optimization design of stabilizing piles in slopes considering spatial variability[J]. Acta Geotechnica, 2020, 15(11): 3243–3259.

[17] LUO Z, HU B. Probabilistic design model for energy piles considering soil spatial variability[J]. Computers and Geotechnics, 2019, 108(APR.): 308–318.

[18] HOEK E, BROWN E T. The Hoek-Brown failure criterion and GSI–2018 edition[J]. Journal of Rock Mechanics and Geotechnical Engineering, 2019, 11(3): 445–463.

[19] WU Shun-chuan, JIN Ai-bing, GAO Yong-tao. Numerical simulation analysis on strength reduction for slope of jointed rock masses based on generalized Hoek-Brown failure criterion[J]. Chinese Journal of Geotechnical Engineering, 2006, 28(11): 1975–1980.

[20] CHEN F, WANG L, ZHANG W. Reliability assessment on stability of tunnelling perpendicularly beneath an existing tunnel considering spatial variabilities of rock mass properties[J]. Tunnelling and Underground Space

Technology, 2019, 88(JUN.): 276–289.

[21] VANMARCKE E H. Probabilistic modeling of soil profiles[J]. Journal of the Geotechnical Engineering Division, 1977, 103(11): 1227–1246.

[22] CHO S E. Probabilistic stability analysis of rainfall-induced landslides considering spatial variability of permeability[J]. Engineering Geology, 2014, 171: 11–20.

[23] CHO S E. Effects of spatial variability of soil properties on slope stability[J]. Engineering Geology, 2007, 92(3–4): 97–109.

[24] Itasca Consulting Group, Inc. FLAC^{3D} (fast Lagrangian analysis of continua in 3D) theory and background[R]. Minneapolis: Itasca Consulting Group, Inc., 2017.

[25] LIU X, WANG Y, LI D Q. Investigation of slope failure mode evolution during large deformation in spatially variable soils by random limit equilibrium and material point methods[J]. Computers and Geotechnics, 2019, 111(JUL.): 301–312.

[26] HAMMAH R E, YACOUB T E, CORKUM B C, et al. The shear strength reduction method for the generalized Hoek-Brown criterion[C]//Proceedings of the 40th U.S. Symposium on Rock Mechanics, Alaska Rocks 2005. Anchorage, Alaska: [s. n.], 2005.

[27] JIANG S H, HUANG J. Modeling of non-stationary random field of undrained shear strength of soil for slope reliability analysis[J]. Soils and Foundations, 2018, 58(1): 185–198.

[28] MAYER J M, STEAD D. A comparison of traditional, step-path, and geostatistical techniques in the stability analysis of a large open pit[J]. Rock Mechanics and Rock Engineering, 2017, 50(4): 927–949.

[29] ÖZTÜRK C A, NASUF E. Geostatistical assessment of rock zones for tunneling[J]. Tunnelling and Underground Space Technology, 2002, 17(3): 275–285.

[30] MAO N, AL-BITTAR T, SOUBRA A H. Probabilistic analysis and design of strip foundations resting on rocks obeying Hoek-Brown failure criterion[J]. International Journal of Rock Mechanics and Mining Sciences, 2012, 49: 45–58.

[31] LÜ Q, XIAO Z, ZHENG J, et al. Probabilistic assessment of tunnel convergence considering spatial variability in rock mass properties using interpolated autocorrelation and response surface method[J]. Geoscience Frontiers, 2018, 9(6): 1619–1629.

[32] AL-BITTAR T, SOUBRA A H. Bearing capacity of spatially random rock masses obeying Hoek-Brown failure criterion[J]. Georisk: Assessment and Management of Risk for Engineered Systems and Geohazards, 2017, 11(2): 215–229.

[33] CHING J, HU Y G, YANG Z Y, et al. Reliability-based design for allowable bearing capacity of footings on rock masses by considering angle of distortion[J]. International Journal of Rock Mechanics and Mining Sciences, 2011, 48(5): 728–740.

[34] ZENG P, SENENT S, JIMENEZ R. Reliability analysis of circular tunnel face stability obeying Hoek-Brown failure criterion considering different distribution types and correlation structures[J]. Journal of Computing in Civil Engineering, 2016, 30(1): 04014126.

[35] YIN Y, LI B, WANG W. Dynamic analysis of the stabilized Wangjiayan landslide in the Wenchuan Ms 8.0 earthquake and aftershocks[J]. Landslides, 2015, 12(3): 537–547.

[36] HALDAR S, BABU G L S. Effect of soil spatial variability on the response of laterally loaded pile in undrained clay[J]. Computers and Geotechnics, 2008, 35(4): 537–547.

[37] ZHU H, ZHANG L M, XIAO T. Evaluating stability of anisotropically deposited soil slopes[J]. Canadian Geotechnical Journal, 2019, 56(5): 753–760.